

# Characterization of voids in shock-loaded Al single crystal by combining X-ray tomography and electron microscopy

**Hong, Chuanshi; Fæster, Søren; Hansen, Niels; Huang, Xiaoxu; Barabash, Rozaliya I.**

*Published in:*
I O P Conference Series: Materials Science and Engineering

*Link to article, DOI:*
10.1088/1757-899X/219/1/012027

*Publication date:*
2017

*Document Version*
Publisher's PDF, also known as Version of record

# Characterization of voids in shock-loaded Al single crystal by combining X-ray tomography and electron microscopy

IOP Conf. Series: Materials Science and Engineering **219** (2017) 012027 doi:10.1088/1757-899X/219/1/012027

# Characterization of voids in shock-loaded Al single crystal by combining X-ray tomography and electron microscopy

**Chuanshi Hong[1,*], Søren Fæster[1], Niels Hansen[1], Xiaoxu Huang[1] and Rozaliya I. Barabash[2]**

[1] Section for Materials Science and Advanced Characterization, Department of Wind Energy, Technical University of Denmark, Risø Campus, 4000 Roskilde, Denmark
[2] Materials Science & Technology Division, Oak Ridge National Laboratory, P.O. Box 2008, Oak Ridge, TN 37830, USA

*E-mail: chho@dtu.dk

**Abstract**. A combination of X-ray tomography and electron backscatter diffraction (EBSD) was applied to investigate both the shape of voids and the plastic deformation around voids in an Al single crystal shock-loaded in the <1 2 3> direction. The combination of these two techniques allows the addition of crystallographic information to X-ray tomography and allows the addition of three-dimensional information to EBSD data. It is found that the voids are octahedral with {1 1 1} faces and that regular patterns of lattice reorientation exist around individual voids. The results provide new insights to the process of void growth during shock loading, which is important for both civil and military applications.

## 1. Introduction

Ductile fracture of metals characterizes their mechanical behavior and is of importance for their application in society. Ductile fracture is known to occur via nucleation, growth and coalescence of voids [1–3], phenomena which have been investigated by analytical and numerical modelling. Modeling of void growth on the continuum level has been well documented [4–9], from which void shape and plastic anisotropy are two factors known to affect void growth to the first order. Atomic simulations have shown that void growth is governed by dislocation slip [10–14]. Experiments on void growth have traditionally focused on the measurement of statistical quantities, such as void sizes and void volume fraction [15–18], whereas experimental insights on the underlying mechanisms are scant.

In the present work we applied a unique combination of X-ray tomography and electron backscatter diffraction (EBSD) to investigate voids in an Al single crystal shock loaded in the <1 2 3> orientation. This crystal has been examined previously by polychromatic X-ray microdiffraction [19]. In the present study new insights were obtained by combining three-dimensional (3D) information (tomography) with a crystallographic analysis in two dimensions (EBSD).

## 2. Experimental

Shock loading of the Al single crystal was performed using a gas gun assembly [19,20]. The initial dislocation density of the crystal was less than $10^7$ $cm^{-2}$ as measured by X-ray diffraction, which is typical of nearly perfect metallic single crystals. The crystal, in the form of a disk of 25 mm in diameter and 5 mm in thickness, was shock loaded in the <1 2 3> direction, parallel to the axis of the

disk. The impact velocity was 165 $m \cdot s^{-1}$ and corresponds to a strain rate of the magnitude of $10^5$ $s^{-1}$ and a pressure in the range of 10–20 GPa.

Characterization of the shock loaded sample was carried out on a core disk of 5 mm in diameter cut from the center of the initial disk. X-ray tomography was carried out using a Zeiss Xradia 520 Versa micro-CT (computerized tomography) system. A polychromatic conical beam with X-ray energies up to 140 keV was used for the CT scans. In total 1401 image projections were recorded over a rotation of 360° during the scan. EBSD samples were prepared in the section containing the axis of the core disk. The samples were mechanically polished and then electro-polished. EBSD was conducted using a Zeiss Supra 35 scanning electron microscope, operated at a high tension of 20 kV and with a mapping carried out using a step size of 0.5 μm.

## 3. Results and analysis

Due to the impact loading, micro voids form in a spall region at about one third the thickness of the sample from the rear surface of the sample. The voids are already visible in the metallographic section as shown in figure 1a. X-ray tomography (figure 1b) reveals that the voids distribute rather homogeneously in the spall region, and that the diameters of voids range from a few to a few hundred micrometers with the mode of the size distribution being about 65 μm. The formation of spallation voids under shock is well known to be a result of the interaction of shock waves.

Remarkably, the voids consistently show the shape of an octahedron with somewhat rounded edges and vertices (figure 1c). By combining X-ray tomography with EBSD, the geometry of the void shape was measured in the coordinate system of the single crystal, revealing that the faces of the octahedral voids are on {1 1 1} planes of the single crystal and that the axes connecting opposite vertices of the octahedrons are along the <1 0 0> directions.

Regular patterns of lattice reorientation were detected on the metallographic section examined by EBSD (figure 2). Morphologically, the reorientation patterns can be classified into four groups. In two groups (figure $2a_1$ and $b_1$), a void is visible in the center of the each reorientation pattern. The morphology of the patterns in these two groups is essentially the same but are inverted (i.e. rotated by 180° around the normal of the EBSD section) relative to each other. In the other two groups (figure $2c_1$ and $d_1$), the patterns are observed on a smooth surface without visible voids. The morphology of these two groups also exhibits 180° rotational symmetry.

Each reorientation pattern is composed of zones of different rotations. In figure $2a_1$ of the first group, sixteen zones are identified, as labelled 0–15. Significant lattice rotation relative to the mean matrix orientation is observed in all identified zones except for Zone 0, where the rotation is negligible. A similar magnitude of lattice rotation is observed for Zones 1–15. The direction of lattice rotation is illustrated by spin rotors in figure $1a_2$. It is mainly the difference in the rotation direction that distinguishes the zones, which is generally larger than 90° between neighboring zones. The zones are located with mirror symmetry about the bisector of the vertex angle of the isosceles shape of the sectioned void (i.e. the vertex angle near Zone 0). The rotation axes in mirrored zones are mirrored-and-inverted relative to each other.

The reorientation pattern in figure $2b_1$ and $b_2$ of the second group has all the characteristics described above for the pattern of the first group. All zones in figure $2a_1$ have counterparts in figure $2b_1$. The direction of lattice rotation in each zone in figure $2b_1$ is largely the same as that of the counterpart zone in figure $2a_1$.

The reorientation patterns in figure $2c_1$ and $d_1$ have an apparent three-fold symmetry. Three pairs of zones are identified in each pattern, labelled as 1–2, 3–4 and 5–6, which are bounded by three high angle boundaries. The three boundaries coincide with the {1 1 0} traces of the mean matrix orientation. As shown in figure $2c_2$ and $d_2$, the direction of lattice rotation changes substantially between neighboring zones of the different pairs bordered by high angle boundaries.

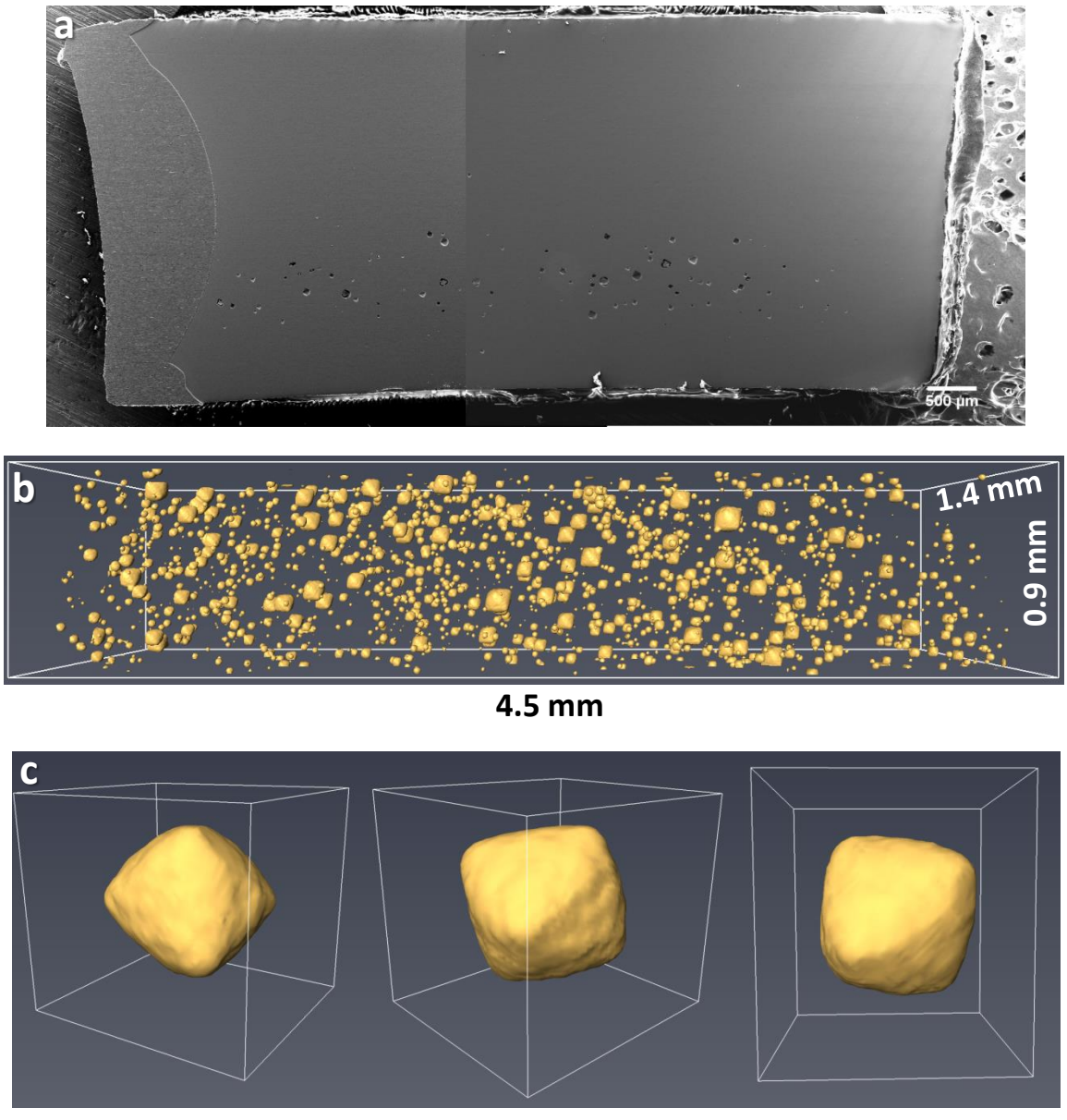


**Figure 1.** (a) A secondary electron image showing the cross-section of the shock-loaded sample. The shock direction is vertical. (b) Reconstruction of voids in the spall region. (c) Close-ups of a single void viewed along different directions.

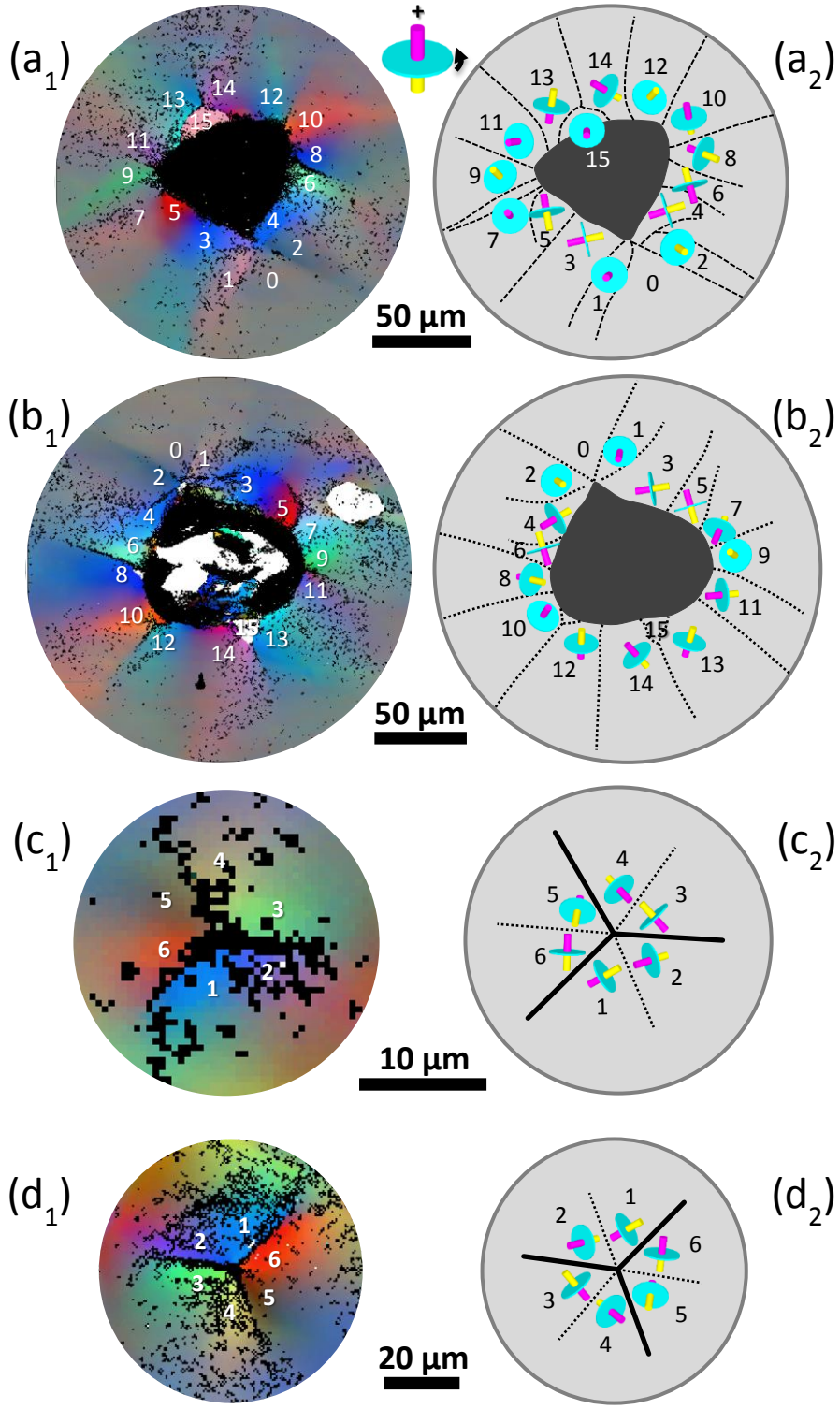


**Figure 2.** Examples of the four typical morphologies of lattice reorientation patterns observed on the cross-section in figure 1a. ($a_1$–$d_1$) EBSD maps (Euler angle coloring). The numbers indicate individual zones of lattice reorientation. ($a_2$–$d_2$) Axes of lattice rotation relative to the mean matrix orientation in each individual zone, illustrated by spin-rotors in the sketches of the reorientation patterns. The positive direction of the spin-rotors is defined by the inset between ($a_1$) and ($a_2$). The solid lines mark visible boundaries and the dashed lines mark approximately the borders of neighboring zones.

A void in the shape of an octahedron is expected to have different profiles on a metallographic section depending on the sectioning plane and position. Figure 3 shows the profile of a reconstructed void on a section parallel to the EBSD section as a function of the sectioning position. A profile of the void similar to figure $2b_1$ is obtained when the void is sectioned at the upper half, and one similar to figure $2a_1$ is obtained when the void is sectioned at the lower half.

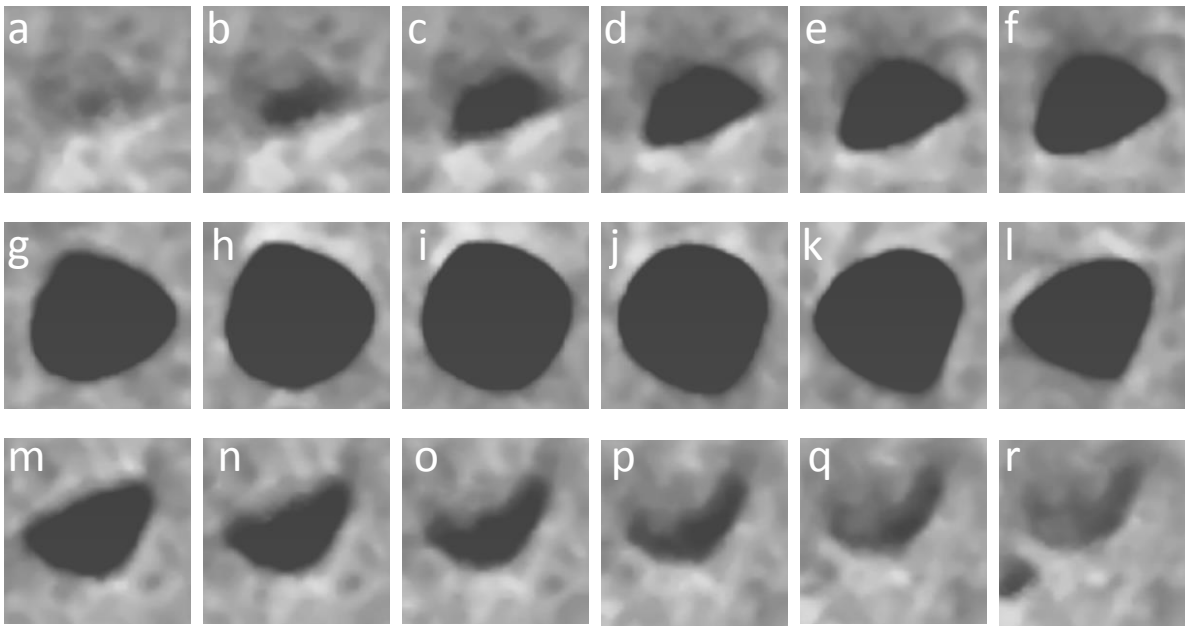


**Figure 3.** (a–r) Evolution of the sectioned morphology of a void as the virtual section (which is parallel to the EBSD section) moves through a void in the 3D reconstruction.

Moreover, the four voids associated with the four reorientation patterns in figure 2, and the exact position of the EBSD section, were identified in the three dimensional (3D) reconstruction (figure 4a). It is therefore concluded that the four reorientation patterns shown in figure 2 correspond to voids sectioned at typical positions, as summarized in figure 4b.

## 4. Discussion

The combination of X-ray tomography and EBSD provides an integrated approach for 3D characterization of voids with crystallographic information. On one hand, EBSD provides crystallographic information for volumes sampled by X-ray tomography. On the other hand, X-ray tomography provides the missing information in the third dimension conventional EBSD on 2D sections. Combined the two techniques allows the four groups of reorientation patterns to be unified. This combination of techniques provides an approach for 3D characterization that is less resource demanding compared 3D XRD techniques or serial-sectioning EBSD, and is in particular suitable for studies of single crystals.

The unique approach employed in the present work shows novel results on void growth. The 3D shape of the void is clearly shown to be crystallographic in the present work, which validates previous results on void shape in two dimensions [1,21–23]. Although X-ray tomography has been used to investigate voids [16–18,24,25], the focus was on statistical quantities, such as void sizes and volume fraction, and only limited attention was paid to the shape of individual voids. Recently, octahedral voids were observed by X-ray tomography in a polycrystalline material [26], but no effort was made to determine the crystallographic characteristics of their shape. Regular reorientation patterning around

voids growing inside a metal matrix during ductile fracture has not been reported previously, although a high density of dislocations or a large magnitude of lattice rotations around voids have been shown by a few experiments [1,19,22,26].

The formation of a crystallographic octahedral shape of the voids is believed to be caused by the anisotropy of plastic flow related to active slip systems in the original single crystal. It is suggested that a highly symmetric configuration of active slip systems is needed for the evolution of the voids into such a shape, which is consistent with the EBSD results. Lattice rotation during plastic deformation is well known to be determined by dislocation slip. The systematic variation in the rotation direction in individual zones in the reorientation patterns indicates a systematic variation of active slip systems. The regular reorientation patterns with 3D symmetry indicate a highly symmetric configuration of these systems. An in-depth analysis of the reorientation patterning based on active slip systems can be found in [27], also including a TEM characterization and a preliminary analysis of the dislocation structures in the reoriented zones around voids.

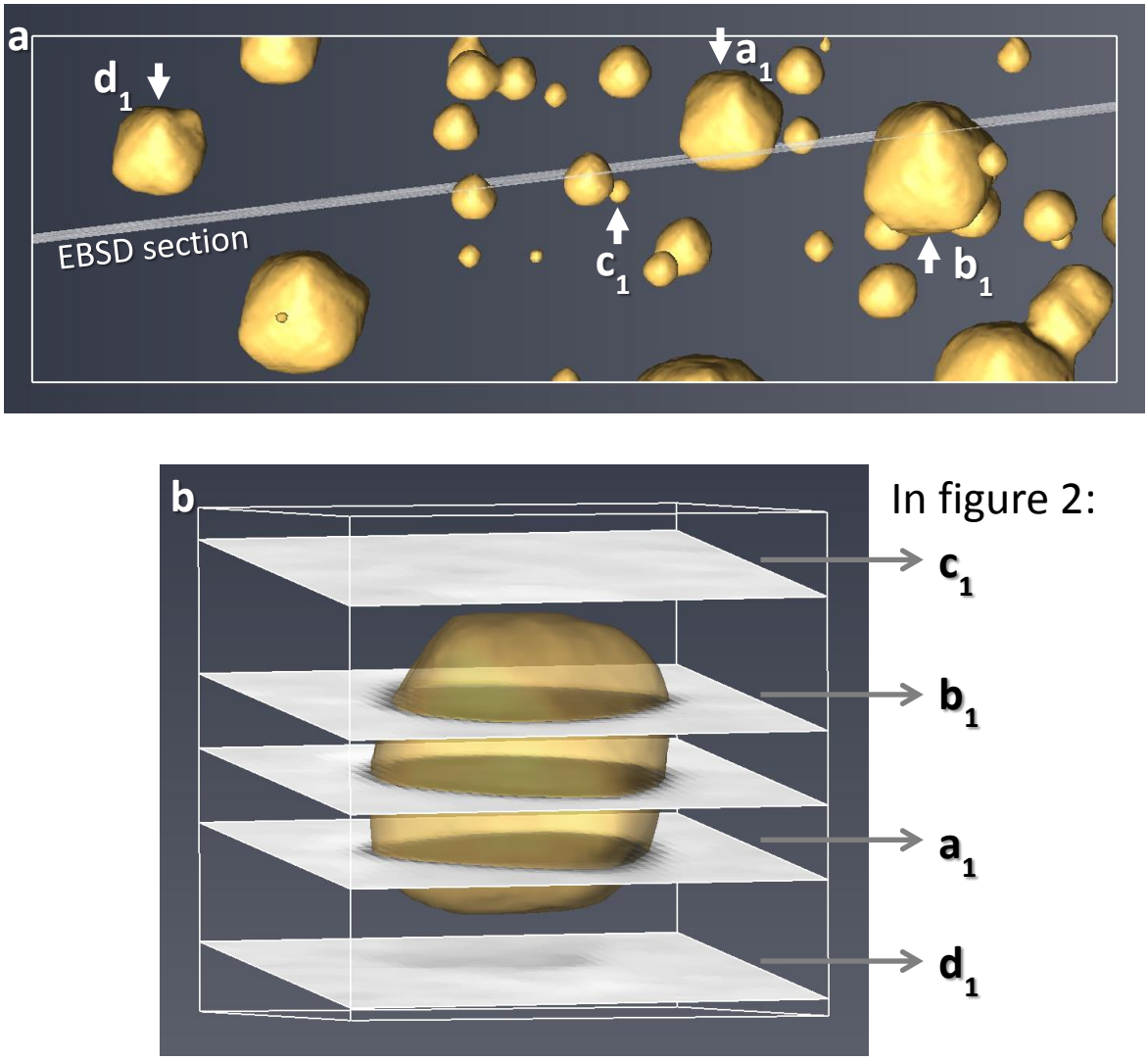


**Figure 4.** (a) Voids associated with the four reorientation patterns, $a_1$, $b_1$, $c_1$ and $d_1$ in figure 2, identified in the 3D reconstruction. The exact position of the EBSD section in the 3D reconstruction is also displayed. (b) Summary of the relation between the sectioning position relative to the void and the reorientation patterns observed in figure 2.

## 5. Conclusions

By combining X-ray tomography and EBSD, a unique approach has been applied in the present work to investigate both the void shape and the pattern of lattice reorientation around voids in a shock-loaded Al single crystal. The approach allows the void shape observed by X-ray tomography to be related to crystallography, and allows the positions of individual voids associated with the lattice reorientation patterns observed in EBSD to be determined, based on which the following can be concluded:

1) The voids have a consistent octahedral shape with faces parallel to the {1 1 1} planes of the single crystal.

2) Regular patterns of lattice reorientation exist around the voids. The patterns consist of zones of large lattice rotation with high angle boundaries between some neighboring zones.

3) The lattice reorientation patterns can be classified into four groups based on morphology, which is an artefact of sectioning of the same 3D reorientation pattern at different positions.

4) The analysis underpins basic and engineering studies of ductile fracture caused by shock loading (strain rate ~$10^5$ $s^{-1}$), important for both civil and military applications of metallic components.

## 6. References

[1] Meyers M A and Taylor Aimone C 1983 Dynamic fracture (spalling) of metals *Prog. Mater. Sci.* **28** 1–96
[2] Garrison W M and Moody N R 1987 Ductile fracture *J. Phys. Chem. Solids* **48** 1035–74
[3] Benzerga A, Leblond J-B, Needleman A and Tvergaard V 2016 Ductile Failure Modeling *Int. J. Fract.* **201** 29–80
[4] Tvergaard V 1981 Influence of voids on shear band instabilities under plane strain conditions *Int. J. Fract.* **17** 389–407
[5] Tvergaard V 1989 Material Failure by Void Growth to Coalescence *Adv. Appl. Mech.* **27** 83–151
[6] Lemaitre J 1985 A Continuous Damage Mechanics Model for Ductile Fracture *J. Eng. Mater. Technol.* **107** 83–9
[7] Castañeda P P and Zaidman M 1994 Constitutive models for porous materials with evolving microstructure *J. Mech. Phys. Solids* **42** 1459–97
[8] Benzerga A A and Leblond J-B 2010 Ductile Fracture by Void Growth to Coalescence *Advances in Applied Mechanics* vol 44pp 169–305
[9] Tvergaard V and Needleman A 1984 Analysis of the cup-cone fracture in a round tensile bar *Acta Metall.* **32** 157–69
[10] Lubarda V A, Schneider M S, Kalantar D H, Remington B A and Meyers M A 2004 Void growth by dislocation emission *Acta Mater.* **52** 1397–408
[11] Tang Y, Bringa E M and Meyers M A 2012 Ductile tensile failure in metals through initiation and growth of nanosized voids *Acta Mater.* **60** 4856–65
[12] Rudd R E 2009 Void growth in bcc metals simulated with molecular dynamics using the Finnis–Sinclair potential *Philos. Mag.* **89** 3133–3161
[13] Marian J, Knap J and Ortiz M 2005 Nanovoid deformation in aluminum under simple shear *Acta Mater.* **53** 2893–900
[14] Marian J, Knap J and Ortiz M 2004 Nanovoid Cavitation by Dislocation Emission in Aluminum *Phys. Rev. Lett.* **93** 165503-1–4
[15] Benzerga A A, Besson J and Pineau A 2004 Anisotropic ductile fracture: Part I: experiments *Acta Mater.* **52** 4623–38
[16] Maire E, Bordreuil C, Babout L and Boyer J-C 2005 Damage initiation and growth in metals. Comparison between modelling and tomography experiments *J. Mech. Phys. Solids* **53** 2411–34
[17] Ueda T, Helfen L and Morgeneyer T F 2014 In situ laminography study of three-dimensional individual void shape evolution at crack initiation and comparison with Gurson-Tvergaard-Needleman- type simulations *Acta Mater.* **78** 254–70

[18] Lieberman E J, Lebensohn R A, Menasche D B, Bronkhorst C A and Rollett A D 2016 Microstructural effects on damage evolution in shocked copper polycrystals *Acta Mater.* **116** 270–80
[19] Barabash R I, Ice G E, Kumar M, Ilavsky J and Belak J 2009 Polychromatic microdiffraction analysis of defect self-organization in shock deformed single crystals *Int. J. Plast.* **25** 2081–93
[20] Gray G T 1993 Influence of Shock-Wave Deformation on the Structure/Property Behavior of Materials *High-Pressure Shock Compression of Solids* (New York, NY: Springer New York) pp 187–215
[21] Stevens A L, Davison L and Warren W E 1972 Spall fracture in aluminum monocrystals: a dislocation-dynamics approach *J. Appl. Phys.* **43** 4922
[22] Perez-Bergquist A G, Cerreta E K, Trujillo C P, Cao F and Gray G T 2011 Orientation dependence of void formation and substructure deformation in a spalled copper bicrystal *Scr. Mater.* **65** 1069–72
[23] Crépin J, Bretheau T and Caldemaison D 1996 Cavity growth and rupture of β-treated zirconium: A crystallographic model *Acta Mater.* **44** 4927–35
[24] Maire E, Bouaziz O, Di Michiel M and Verdu C 2008 Initiation and growth of damage in a dual-phase steel observed by X-ray microtomography *Acta Mater.* **56** 4954–64
[25] Bingert J F, Henrie B L and Worthington D L 2007 Three-Dimensional Characterization of Incipiently Spalled Tantalum *Metall. Mater. Trans. A* **38** 1712–21
[26] Qi M L, Yao Y, Bie B X, Ran X X, Ye W, Fan D and Li P 2015 Nucleation and growth of damage in polycrystalline aluminum under dynamic tensile loading *AIP Adv.* **5** 37116
[27] Hong C, Fæster S, Hansen N, Huang X and Barabash R I 2017 Non-spherical voids and lattice reorientation patterning in a shock-loaded Al single crystal, *Acta Mater. in press*